GNAQ/GNA11 Mosaicism Is Associated with Abnormal Serum Calcium Indices and Microvascular Neurocalcification

TITLE

GNAQ/GNA11 mosaicism is associated with abnormal serum calcium indices and microvascular neurocalcification

AUTHORS

Nicole Knöpfel[1,2,3*], Davide Zecchin[1,2*], Hanna Richardson[4], Satyamaanasa Polubothu[1,2,3], Sara Barberan-Martin[1,2], Thomas Cullup[5], Karolina Gholam[3], Simon Heales[6], Steve Krywawych[6], Pablo López-Balboa[3], Noreen Muwanga-Nanyonjo[1,2], Olumide Ogunbiyi[7], Clinda Puvirajasinghe[5], Lea Solman[3], Katherine Swarbrick[7], Samira B. Syed[3], Zubair Tahir[8], Martin M. Tisdall[8], Jeremy Allgrove[9], Alexander D. Chesover[9], Sarah E. Aylett[4], Thomas S. Jacques[7,10], Fadil M. Hannan[11], Ulrike Löbel[12], Robert K. Semple[13], Rajesh V. Thakker[14,15], Veronica A. Kinsler[1,2,3]

ORCIDs

Nicole Knöpfel: 0000-0002-6438-6550; Davide Zecchin: 0000-0002-4784-0336; Hanna Richardson:0009-0005-5589-8027; Satyamaanasa Polubothu: 0000-0001-7195-5670; Sara Barberan-Martin: 0000-0003-0142-4078; Thomas Cullup: 0009-0009-9850-0698; Karolina Gholam: 0000-0002-8109-6993; Simon Heales: 0000-0002-9906-0200; Steve Krywawych: 0009-0000-9161-5550; Pablo López-Balboa: 0000-0002-9944-719X; Noreen Muwanga-Nanyonjo: 0009-0005-4772-4748; Olumide Ogunbiyi: 0000-0001-5208-5526; Clinda Puvirajasinghe: 0000-0003-1646-6588; Lea Solman: 0000-0002-6183-6608; Samira B. Syed: 0000-0002-3872-5870; Zubair Tahir: 0000-0001-9797-3770; Martin M. Tisdall: 0000-0001-8880-8386; Jeremy Allgrove: 0000-0003-0858-7064; Alexander D. Chesover: 0000-0002-6280-5053; Sarah E. Aylett: 0000-0001-9630-3222; Thomas S. Jacques: 0000-0002-7833-2158; Fadil M. Hannan: 0000-0002-2975-5170; Ulrike Löbel: 0000-0001-9844-3464; Robert

K. Semple: 0000-0001-6539-3069; Rajesh V. Thakker: 0000-0002-1438-3220; Veronica A. Kinsler: 0000-0001-6256-327

AFFILIATIONS

1. Mosaicism and Precision Medicine Laboratory, Francis Crick Institute; London NW1 1AT, UK
2. Genetics and Genomic Medicine, UCL GOS Institute of Child Health; London WC1N 1EH, UK
3. Department of Paediatric Dermatology, Great Ormond St Hospital for Children; London WC1N 3JH, UK
4. Neurodisability, Great Ormond St Hospital for Children; London WC1N 3JH, UK
5. North Thames Genomic Laboratory Hub, Levels 4-6, Barclay House, Great Ormond St Hospital for Children NHS Foundation Trust; London WC1N 3BH, UK
6. Department of Chemical Pathology NIHR BRC, Great Ormond St Hospital for Children NHS Foundation Trust; London WC1N 3JH, UK.
7. Department of Histopathology, Great Ormond St Hospital for Children NHS Foundation Trust; London WC1N 3JH, UK
8. Paediatric Neurosurgery, Great Ormond St Hospital for Children NHS Foundation Trust; London WC1N 3JH, UK
9. Endocrinology, Great Ormond St Hospital For Children NHS Foundation Trust; London WC1N 3JH, UK.
10. Developmental Biology and Cancer Programme, UCL GOS Institute of Child Health; London, UK
11. Nuffield Department of Women's & Reproductive Health, University of Oxford; Oxford, United Kingdom

12. Radiology, Great Ormond St Hospital for Children; London WC1N 3JH, UK
13. Centre for Cardiovascular Science, Queen's Medical Research Institute, University of Edinburgh; Edinburgh, UK
14. Academic Endocrine Unit, Radcliffe Department of Medicine,University of Oxford; Oxford OX3 7LJ, UK
15. National Institute for Health Research Oxford Biomedical Research Centre; Oxford, UK

***These authors share first authorship**

CORRESPONDING AUTHOR

Veronica Kinsler, Mosaicism and Precision Medicine Laboratory, Francis Crick Institute, London, UK; Tel: +442037965396; Email: v.kinsler@ucl.ac.uk

SHORT TITLE

GNAQ/GNA11 mosaicism is associated with abnormal serum calcium

ABBREVIATIONS

SWS: Sturge-Weber syndrome; PPV-DM: Phakomatosis Pigmentovascularis types associated with dermal melanocytosis; SEM: standard error of the mean; PTH: parathyroid hormone; ALP: alkaline phosphatase; iFGF23: intact fibroblast growth factor 23; cFGF23: C-terminal fibroblast growth factor 23; TRP: tubular reabsorption of phosphate; E-GFR estimated glomerular filtration rate; CT: computed tomography; MRI: magnetic resonance imaging;

ABSTRACT

Mosaic mutations in genes *GNAQ* or *GNA11* lead to a spectrum of diseases including Sturge-Weber syndrome (SWS) and phakomatosis pigmentovascularis with dermal melanocytosis (PPV-DM). The pathognomonic finding of localised "tramlining" on plain skull radiography, representing medium-sized neurovascular calcification and associated with post-natal neurological deterioration, led us to study calcium metabolism in a cohort of 42 children. We find here that 74% of patients had at least one abnormal measurement of calcium metabolism, the commonest being moderately low serum ionised calcium (41%) or high PTH (17%). Lower levels of ionised calcium even within the normal range were significantly associated with seizures, and with specific anti-epileptics despite normal vitamin D levels. Successive measurements documented substantial intrapersonal fluctuation in indices over time, and DEXA scans were normal in hypocalcaemic patients. Neurohistology from epilepsy surgery in five patients revealed not only intravascular, but perivascular and intraparenchymal mineral deposition and intraparenchymal microvascular disease in addition to previously reported findings. Neuroradiology review clearly demonstrated progressive calcium deposition in individuals over time. These findings and those of the adjoining paper suggest that calcium deposition in the brain of patients with *GNAQ/GNA11* mosaicism may not be the non-specific sign of damage it was previously thought, but may instead reflect the central post-natal pathological process in this disease spectrum.

INTRODUCTION

With the discovery of many of the causal genes, complex phenotypic classifications of mosaic disorders affecting the skin have now been grouped together as disease spectra. The spectrum of *GNAQ*/*GNA11* mosaicism essentially encompasses variable combinations of vascular and/or pigmentary abnormalities variably affecting the skin, eyes and brain (**Fig.1**). Well-defined phenotypes include Sturge-Weber syndrome (SWS, purely vascular) and phakomatosis pigmentovascularis with dermal melanocytosis (PPV-DM, vascular and pigmentary). For a full description of the phenotypic variability in this spectrum we refer the reader to previous publications(Polubothu et al., 2020, Shirley et al., 2013, Sliepka et al., 2019, Thomas et al., 2016).

The neurovascular abnormalities in *GNAQ/GNA11* mosaicism present with seizures, neurodevelopmental impairment, headaches and stroke-like episodes(Comi, 2007), which progress post-natally. The original, classical and pathognomonic finding associated with neurovascular disease is neurovascular calcification, first seen on plain skull radiography where the parallel lines of calcification of affected blood vessel walls were described as "tramlining"(Weber, 1922) (**Fig.1f-g**). This tramlining was in fact visualisation of calcified mediumsized veins within the soft leptomeningeal coverings of the brain. Despite its pathognomonic nature, and in particular its absence from other mosaic vascular malformations in the brain, this feature has been considered to be a non-specific marker of tissue damage(Bostrom et al., 1993). With the advent of increasingly advanced imaging techniques, neuropathology in *GNAQ/GNA11* mosaicism has concluded that slow blood flow through the leptomeningeal vascular malformations leads to underlying parenchymal hypoxia and hence neurological deterioration over time(Kelley et al., 2005, Lin et al., 2006, Pilli et al., 2017). Interestingly, both the degree of intracranial calcification and the degree of venous

hypoperfusion on radiological studies have been correlated with neurological symptoms(Kelley et al., 2005, Lin et al., 2006, Pilli et al., 2017). These facts suggested to us that the calcification may be central to the process of neurological deterioration, and may be a clue to the localised vascular biological abnormalities.

Calcium is a critical component of transmembrane and intracellular signalling(Bootman et al., 2001). As such, serum calcium levels are tightly controlled by homeostatic mechanisms involving parathyroid hormone (PTH) and Vitamin D(Goltzman et al., 2018), and these mechanisms will prioritise serum calcium levels over for example bone health. Inherited monogenic diseases affecting calcium metabolism such as Familial Hypocalciuric Hypercalcemia (FHH) and Pseudohypoparathyroidism (PHP) types 1A and 1B are well-documented to lead to intravascular calcification(Iwase et al., 2019, Pollak et al., 1993). Mosaic disorders however, although monogenic, only affect some parts of the body, and in this regard could conceivably behave more like multiple tumour foci than a genetic disease. We therefore hypothesised that the known neurovascular calcification could be related to abnormal calcium fluxes in and around foci of affected blood vessels, and that this could potentially affect serum calcium levels. We further hypothesised that microvascular calcification could be an undocumented aspect of disease that could lead to brain tissue hypoxia, independent of leptomeningeal involvement. As a result we undertook a large cross-sectional study of children with diagnoses in the *GNAQ/GNA11* mosaicism spectrum, to determine their calcium metabolic profile in addition to deep clinical phenotyping and offering genotyping. In parallel we reviewed all available neuroimaging and neurohistology, particularly to characterise the neurocalcification.

RESULTS

SWS/PPV-DM cohort has classical neuroradiological and clinical progression and genotypic profile

Forty-two patients were recruited, 21 female, 31 with SWS, two with extensive cutaneous capillary malformations and nine with PPV-DM (**Fig. 1a-c**). Mean and median ages were 7.62 (standard error of the mean SEM 0.76) and 8 years respectively (range 0.2-16.1). Phenotypic, genotypic and results data are summarised in **Table 1**, and a key finding was a mean and median age of onset of seizures of 0.98 years (SEM 0.25) and 0.63 (range 0-5.92) respectively, confirming the post-natal deterioration described in previous studies. Intracranial calcifications were detectable on imaging in 50% of patients (**Fig. 1f,g**). Neurovascular calcification was clearly demonstrated to develop over time where multiple scans were available from the same patient (**Fig. 1h-k**). Genotyping was accepted by 29 patients and results were representative of previous cohort publications(Jordan et al., 2020, Polubothu et al., 2020, Shirley et al., 2013). The pathogenic variants underlying the clinical diagnoses were identified as follows: SWS caused by a mosaic variant in *GNAQ* c.548G>A, p.(R183Q) in 17 patients; widespread CM only caused by *GNA11* c.547C>T, p.(R183C) in one; PPV-DM caused by *GNAQ* c.548G>A, p.(R183Q) in three and by *GNA11* c.547C>T, p.(R183C) in another five. Three patients (two SWS and one PPV-DM) were double-WT.

SWS/PPV patients have fluctuating levels of serum ionised calcium with normal 25-hydroxy-vitamin D levels

All calcium metabolism-related parameters were measured in the same diagnostic laboratory using age- and gender adjusted reference intervals from the UK normal population. Three patients had low 25-hydroxy-vitamin D on first measurement, and were given oral supplementation and resampled before cohort results were analysed. On that corrected

background, seventy-four percent (31/42) of patients at first sampling had at least one abnormal measurement of calcium metabolism, defined here as pH-corrected ionised calcium, albumin-corrected total calcium, parathyroid hormone (PTH), phosphate, magnesium, 25-hydroxy-vitamin D, alkaline phosphatase (ALP) and urinary calcium:creatinine ratio. The commonest findings were moderately low serum ionised calcium (the active form) in 41% (15/37), high PTH in 17% (7/42), and appropriately adjusted urinary calcium excretion for abnormal serum levels in 17% (5/30). We undertook repeat sampling in 26 and 10 patients (two and three sampling time points respectively) (**Fig. 2a, Table S1**). This demonstrated fluctuating levels of abnormal measurements within patients, but with a similar overall proportion of abnormal results in the cohort at each time point (69% and 80% at sampling points two and three respectively). Mirroring this, expected inter-relationships between parameters – for example inverse levels of serum calcium and of PTH – were not always preserved within an individual at a particular timepoint, however they were clearly related in the normal way when the cohort measurements were considered as a whole (**Fig. S1**). PTH showed the expected inverse correlation with serum Ca (**Fig.S1A**), urine Ca/Cr ratio appropriately increased with increasing serum Ca (**Fig.S1B**).

To attempt to unpick these profiles further, we went on to measure intact and C-terminal fibroblast growth factor 23 (iFGF23 and cFGF23) and 1,25-dihydroxy-vitamin D in those patients who agreed to repeat testing and in whom adequate sample could be obtained (**Table S1**). cFGF23 was high in 9/20 (mean 105.9RU/mL, range 23-355) with normal iFGF23 in 17/18, and normal 1,25-dihydroxyvitamin D and phosphate concentrations. Of note, cFGF23 and iFGF23 levels showed an opposite correlation with different physiological parameters, and only iFGF23 displayed statistical significant negative correlation with 1,25-dihydroxyvitamin D (**Fig. S1**). 1,25-dihydroxyvitamin D was low in 7/20 (mean 129.6pmol/L, range 53-218) ,

all with normal 25-hydroxy-vitamin D levels (**Table S1**). iFGF23 and 1,25D showed the expected inverse correlation (**Fig.S1C**) whereas no correlation was observed between 1,25D and PTH (**Fig.S1D**).

SWS/PPV patients have no major abnormalities of calcium metabolic functioning of parathyroids, kidneys and skeletal systems

Due to the mosaic variability in inter-patient and intra-patient measurements, associations between key calcium metabolic parameters were modelled at cohort level. PTH showed the expected inverse correlation with serum Ca (**Fig. S2a**), urine Ca/Cr ratio appropriately increased with increasing serum Ca (**Fig. S2b**), and iFGF23 and 1,25-dihydroxyvitamin D showed the expected inverse correlation (**Fig. S2c**) whereas no correlation was observed between 1,25-dihydroxyvitamin D and PTH (**Fig. S2d**). This lack of relationship between PTH and 1,25-dihydroxyvitamin D indicates that iFGF23 may be the physiological regulator of 1,25-dihydroxyvitamin D in these patients. Estimated glomerular filtration rate (E-GFR) measurements were normal throughout (**Table S1**), as were blood pressure measurements where available (n=39). Whole body DEXA scans were normal in eleven patients with hypocalcaemia and borderline abnormal when excluding the head in one (Z score =- 1.9).

Serum ionised calcium is significantly inversely associated with seizures, status epilepticus and anti-epileptics

Multiple linear regression modelling of total serum corrected calcium showed a significant negative association with increasing age ($p=0.001$) (**Fig. 2b**) and no association with affected skin surface area. Linear regression of urinary calcium:creatinine ratio by age alone showed the same significant negative association with increasing age ($p=0.001$), as did serum magnesium and phosphate ($p<0.001$ both).

We then modelled the commonest adverse outcome, patient seizures, using the commonest serum abnormality, ionised calcium. This demonstrated a significant inverse association (p=0.013) between serum ph-corrected ionised calcium level and the presence of seizures (**Fig. 2c**), and of status epilepticus (p= 0.017) (**Fig. 2d**). Significant associations between ionised calcium and levetiracetam (p=0.02) and oxcarbazepine (p=0.003) use were also seen (corrected for age in the multiple regression), but not with other antiepileptics (**Table S2**). No association between prophylactic aspirin use and occurrence of seizures was found in this cohort.

For the key abnormal calcium metabolic parameters patient sex did not significantly affect the regression findings. The statistical contribution of different diagnostic labels and of genotype were not modelled given the cohort size but could be of interest in the future.

Histopathology of affected brain sections demonstrates intravascular, perivascular and intraparenchymal mineral deposition, and primarily microvascular disease

Histological sections of cerebral cortex and overlying leptomeninges from five cases of epilepsy surgery were reviewed. All patients had calcification on previous brain imaging. All showed abnormal mineral deposits (**Fig. 3a-d**), classified as very extensive in four and sparse in one, affecting the cortical parenchyma in all, the white matter parenchyma in four, and the leptomeninges in one. There were frequent perivascular deposits (**Fig. 3b,d**), but there was also genuine mineralisation of the walls of both very small (mostly cortical) vessels (presumed capillaries) and small venules/arterioles (usually in the white matter) (**Fig. 3b,c**). In two cases the latter was quite extensive with the vessel encircled by dense mineral. The location of the mineral in the wall was not clear, but in those vessels where a distinction were possible, it appeared to be in the tunica adventitia and media.

In addition, the cases showed typical vascular malformations within the leptomeninges, and two cases showed focal disruption of the normal cortical architecture, a feature previously

recognised in some SWS patients. Additional non-specific neuropathological findings included gliosis and volume loss, demonstrated by sulcal widening.

DISCUSSION

This study began with a reappraisal of the potential pathogenetic relevance of neurovascular calcification as one of the cardinal signs of disease in *GNAQ/GNA11* mosaicism. We have demonstrated clear although moderate abnormalities of calcium metabolic profile in the cohort as a whole, with a tendency to hypocalcaemia. On the basis of normal parathyroids and renal function we considered these could be related to anti-seizure medications, which are commonly understood to cause 25-hydroxy-vitamin D deficiency and resultant calcium metabolic abnormalities(Aksoy et al., 2016, Koo et al., 2013, Nissen-Meyer et al., 2007, Verrotti et al., 2010). In support of this, we identified a significant association between two commonly used anti-seizure medications, levetiracetam and oxcarbazepine, and lower (although not necessarily abnormal) calcium levels. Such a relationship has previously been described in (non-*GNAQ/GNA11*) patients with seizures (Aksoy et al., 2016), however again those patients had low 25-hydroxy-vitamin D, which our patient cohort did not have.

There is therefore either an as yet unknown explanation for their calcium metabolic disturbances, potentially related to the calcium signalling disturbances, or the anti-seizure drug effect on calcium metabolic profiling is not mediated through abnormal 25-hydroxy-vitamin D levels. Independent of the mechanism, the systemic findings may provide an important and to our knowledge previously unreported insight for clinical management of these patients with deteriorating neurology in the first year of life. Calcium is known as a stabiliser of excitable membranes, and although the levels of serum calcium would not be expected to cause seizures

in a healthy individual, in the context of a seizure disorder they could be a contributory factor. Furthermore, due to the demonstrable cellular abnormalities, local levels of extracellular peri-vascular calcium may be much more profoundly depleted, which could have direct local effects on cells in the region of the vascular malformations. At biological level the interaction between severely abnormal cells and normal cell populations in a mosaic disorder can produce unpredictable effects and in this regard mosaic disorders lie closer to tumour-host interactions than to germline monogenic diseases.

Histopathological review here confirms widespread mineral deposits throughout the cortex and white matter, the vascular and perivascular nature of many of the deposits, and the additional presence of intraparenchymal deposits not clearly related to vessels. Whether this is due to obliteration of previous small vessels through the calcification process or to primary parenchymal calcification is not known. Importantly, where the parenchymal calcification is related to vasculature, this is largely microvascular, and therefore similar in nature to the microvascular disease in the skin. This adds an important insight into Sturge-Weber and PPV-DM neurovascular disease, previously considered to be related to larger vessel abnormalities and their effects on underlying cerebral perfusion. Occlusion of microvasculature by progressive mineral deposition could be a critical component of the abnormal cerebral perfusion and the post-natal neurodeterioration typical of the disease. If this is the case, early therapeutic intervention to prevent microvascular calcification could potentially be extremely important, even in the context of irreversible larger vessel malformations.

MATERIALS AND METHODS

Patient cohort

Forty patients with a clinical diagnosis of SWS or PPV-DM and two affected by extensive capillary malformation only were recruited prospectively from a single center with written informed consent by their parents or guardians and under local Research Ethics Committee approval (London Bloomsbury Research Ethics Committee of Great Ormond Street Hospital/UCL Institute of Child Health, London, United Kingdom). Patients and/or parents/guardians provided written consent for the publication of images. SWS and PPV-DM patients have been grouped together as they are part of the spectrum of *GNAQ/GNA11* mosaic disorders and have an identical vascular phenotype and associated clinical phenotype. Clinical and radiological phenotyping of cutaneous, neurological, and ophthalmological manifestations and calcium metabolic profile analysis in blood and urine were undertaken.

Cutaneous features recorded were the presence or absence of capillary malformation (port wine stain with or without naevus anaemicus), dermal melanocytosis, and involvement of the forehead area by vascular and/or pigmentary lesions. The proportion of the body covered by the capillary malformation was estimated using the Lund-Browder chart. Other recorded features were head circumference, overgrowth or undergrowth of other body areas , skeletal and endocrinological abnormalities, blood pressure, neurological and ophthalmological phenotype. Retrospective review of all brain computed tomography (CT, n=7) and magnetic resonance imaging (MRI, n=36) studies, including gradient-echo imaging (i.e. T2*, susceptibility-weighted imaging or the b0 map of the diffusion-weighted sequence, in case the former were not available), was performed by a single radiologist.

All blood sampling was performed in an out-patient setting while the patient was stable. Blood indices measured were ionised calcium, total calcium, phosphate, magnesium, PTH, ALP, FGF23, both cFGF23 and iFGF23 (Immutopics), 1,25-dihydroxyvitamin D, 25-hydroxy-

vitamin D and urea and electrolytes. Urinary calcium:creatinine ratio, tubular reabsorption of phosphate (TRP), ratio of tubular maximum reabsorption of phosphate to glomerular filtration rate (TmP/GFR) and E-GFR were also determined. Patients with serum ionised hypocalcaemia were offered a whole body DEXA scan, performed in 12 cases. Comparison of serum indices was made by reference to the Great Ormond St Hospital reference laboratory standards(Lockitch et al., 1988).

Genotyping of affected tissue by 4mm skin punch biopsy was offered to the entire cohort. DNA was extracted by standard methods from whole skin and underwent targeted panel sequencing for all coding sequences of *GNAQ* and *GNA11* to a mean depth of 1500X using Illumina technology.

Expert neurohistopathological review was undertaken of brain sections from five patients involved in the study in whom epilepsy surgery had previously been performed, using H+E and Elastin Van Gieson staining.

Statistical analysis

Multiple linear regression analysis was performed to model serum corrected calcium and urinary calcium:creatinine ratio each by age, sex, and affected skin area, using SPSS v.28, and with p value significance adjusted for multiple testing. Multiple binary regression was performed to model seizures and status epilepticus against the same independent variables. Correlations between serum parameters were modelled in Prism using simple linear regression analysis and stringency (ROUT Q=1%), which resulted in a single outlier removal from 65 measurements. Removal of the outlier did not alter the significance or otherwise of any of correlations.

Study approval

The study was approved by the London Bloomsbury Research Ethics Committee of Great Ormond Street Hospital/UCL Institute of Child Health (London, United Kingdom). All participants' parents or guardians provided written informed consent for skin biopsy and/or brain tissue sampling for genetic testing and blood/urine investigations. Separate written informed consent was obtained for publication of clinical photographs.

DATA AVAILABILITY STATEMENT

All data are available in the main text or the supplementary materials

CONFLICT OF INTEREST STATEMENT

The authors declare no conflict of interest.

ACKNOWLEDGMENTS

We gratefully acknowledge the participation of the patients and families in this research and research coordination by Jane White. VK and NK are funded by the UK NIHR (grant NIHR300774). This work was supported by the GOSHCC Livingstone Skin Research Centre and by the UK National Institute for Health Research (NIHR) through the Biomedical Research Centre at Great Ormond St Hospital for Children NHS Foundation Trust and the UCL GOS Institute of Child Health. R.V.T. was funded by a grant (106995/Z/15/Z) from the Wellcome Trust, a grant from the Oxford Biomedical Research Centre Program of the National Institute for Health Research (NIHR), a grant (NF-SI-0514–10091) from the NIHR. R.K.S. was funded by a grant (210752/Z/18/Z) from the Wellcome Trust. A.I. was funded by Japan Society for the Promotion of Science (JSPS) KAKENHI grants 21H04791 and 21H05113; Moonshot Research and Development Program JPMJMS2023 from Japan Science and Technology

Agency (JST); the the LEAP JP20gm0010004 and the BINDS JP20am0101095 from the Japan Agency for Medical Research and Development (AMED); Daiichi Sankyo Foundation of Life Science; Takeda Science Foundation; The Uehara Memorial Foundation; The Tokyo Biochemical Research Foundation.

AUTHOR CONTRIBUTIONS

Conceptualization: VK

Data curation: DZ, NK, TJ, RVT, FMH, RKS

Formal analysis: DZ, NK, VK, JA, ADC, TSJ, FMH, RVT

Investigation: DZ, NK, TC, CP, TSJ, UL

Methodology: DZ, NK, VK

Project administration: VK

Resources: NK, HR, SP, SBM, KG, SM, SK, PLB, NMN, OO, LS, LS, SBS, ZT, MT, SEA, UL

Software: NK, DZ

Supervision: VK

Validation: NK, DZ

Visualization: DZ, NK, TSJ, UL

Writing – original draft: NK, DZ

Writing – review & editing: VK, FMH, RVT

REFERENCES

Aksoy D, Guveli BT, Ak PD, Sari H, Atakli D, Arpaci B. Effects of Oxcarbazepine and Levetiracetam on Calcium, Ionized Calcium, and 25-OH Vitamin-D3 Levels in Patients with Epilepsy. Clin Psychopharmacol Neurosci 2016;14(1):74-8.

Bootman MD, Collins TJ, Peppiatt CM, Prothero LS, MacKenzie L, De Smet P, et al. Calcium signalling--an overview. Semin Cell Dev Biol 2001;12(1):3-10.

Bostrom K, Watson KE, Horn S, Wortham C, Herman IM, Demer LL. Bone morphogenetic protein expression in human atherosclerotic lesions. J Clin Invest 1993;91(4):1800-9.
Comi AM. Sturge-Weber syndrome and epilepsy: an argument for aggressive seizure management in these patients. Expert Rev Neurother 2007;7(8):951-6.
Goltzman D, Mannstadt M, Marcocci C. Physiology of the Calcium-Parathyroid Hormone-Vitamin D Axis. Front Horm Res 2018;50:1-13.
Iwase T, Yoshida M, Hashizume Y, Yazawa I, Takahashi S, Ando T, et al. Intracranial vascular calcification with extensive white matter changes in an autopsy case of pseudopseudohypoparathyroidism. Neuropathology 2019;39(1):39-46.
Jordan M, Carmignac V, Sorlin A, Kuentz P, Albuisson J, Borradori L, et al. Reverse Phenotyping in Patients with Skin Capillary Malformations and Mosaic GNAQ or GNA11 Mutations Defines a Clinical Spectrum with Genotype-Phenotype Correlation. The Journal of investigative dermatology 2020;140(5):1106-10 e2.
Kelley TM, Hatfield LA, Lin DD, Comi AM. Quantitative analysis of cerebral cortical atrophy and correlation with clinical severity in unilateral Sturge-Weber syndrome. J Child Neurol 2005;20(11):867-70.
Koo DL, Joo EY, Kim D, Hong SB. Effects of levetiracetam as a monotherapy on bone mineral density and biochemical markers of bone metabolism in patients with epilepsy. Epilepsy Res 2013;104(1-2):134-9.
Lin DD, Barker PB, Hatfield LA, Comi AM. Dynamic MR perfusion and proton MR spectroscopic imaging in Sturge-Weber syndrome: correlation with neurological symptoms. J Magn Reson Imaging 2006;24(2):274-81.
Lockitch G, Halstead AC, Albersheim S, MacCallum C, Quigley G. Age- and sex-specific pediatric reference intervals for biochemistry analytes as measured with the Ektachem-700 analyzer. Clin Chem 1988;34(8):1622-5.
Nissen-Meyer LS, Svalheim S, Tauboll E, Reppe S, Lekva T, Solberg LB, et al. Levetiracetam, phenytoin, and valproate act differently on rat bone mass, structure, and metabolism. Epilepsia 2007;48(10):1850-60.
Pilli VK, Behen ME, Hu J, Xuan Y, Janisse J, Chugani HT, et al. Clinical and metabolic correlates of cerebral calcifications in Sturge-Weber syndrome. Developmental medicine and child neurology 2017;59(9):952-8.
Pollak MR, Brown EM, Chou YH, Hebert SC, Marx SJ, Steinmann B, et al. Mutations in the human Ca(2+)-sensing receptor gene cause familial hypocalciuric hypercalcemia and neonatal severe hyperparathyroidism. Cell 1993;75(7):1297-303.
Polubothu S, Al-Olabi L, Carmen Del Boente M, Chacko A, Eleftheriou G, Glover M, et al. GNA11 Mutation as a Cause of Sturge-Weber Syndrome: Expansion of the Phenotypic Spectrum of Galpha/11 Mosaicism and the Associated Clinical Diagnoses. J Invest Dermatol 2020;140(5):1110-3.
Shirley MD, Tang H, Gallione CJ, Baugher JD, Frelin LP, Cohen B, et al. Sturge-Weber syndrome and port-wine stains caused by somatic mutation in GNAQ. N Engl J Med 2013;368(21):1971-9.
Sliepka JM, McGriff SC, Rossetti LZ, Bizargity P, Streff H, Lee YS, et al. GNA11 brain somatic pathogenic variant in an individual with phacomatosis pigmentovascularis. Neurol Genet 2019;5(6):e366.
Thomas AC, Zeng Z, Riviere JB, O'Shaughnessy R, Al-Olabi L, St-Onge J, et al. Mosaic Activating Mutations in GNA11 and GNAQ Are Associated with Phakomatosis Pigmentovascularis and Extensive Dermal Melanocytosis. J Invest Dermatol 2016;136(4):770-8.
Verrotti A, Coppola G, Parisi P, Mohn A, Chiarelli F. Bone and calcium metabolism and antiepileptic drugs. Clin Neurol Neurosurg 2010;112(1):1-10.

Waelchli R, Aylett SE, Robinson K, Chong WK, Martinez AE, Kinsler VA. New vascular classification of port-wine stains: improving prediction of Sturge-Weber risk. Br J Dermatol 2014;171(4):861-7.

FIGURE LEGENDS

Figure 1 - **Phenotyping and radiological findings in *GNAQ/GNA11* mosaicism. (a)** Clinical features of a SWS syndrome patient with a capillary malformation of the head involving the critical forehead area, associated with glaucoma in the right eye. This patient had hypocalcaemia with low levels of ionised and total calcium and increased PTH. **(b and c)** Clinical features of a PPV-DM patient exhibiting a capillary malformation (with naevus anaemicus) on the face, upper trunk and extensive areas of dermal melanocytosis. **(d** and **e)** Contrast enhanced FLAIR and T1-weighted MR images of a patient with SWS show left frontal, parietal and occipital pial angiomatosis (vascular malformation, arrows). **(f)** Susceptibility-weighted imaging (SWI) and (**g**) SWI phase map depicting vascular calcifications (arrow). This patient had low levels of ionised calcium and total calcium with PTH in the normal range. **(h)** Axial DWI b0 image does not show calcifications on the initial MRI study. **(i-k)**, after 8 years time. **(i)** Coronal Fluid-attenuated inversion recovery (FLAIR) after administration of a gadolinium-based contrast agent shows left parietal and occipital (and some contralateral) sulcal enhancement in keeping with pial angioma. **(j)** Axial post-contrast T1-weighted image depicts the sulcal enhancement and a prominent draining vein. **(k)**. DWI b0 image at follow-up shows foci of increased susceptibility which are suggestive of calcification. Patients and/or parents/guardians provided written consent for the publication of images.

Figure 2 **- Disruption of calcium homeostasis in patients with *GNAQ/GNA11* mosaicism and its association with seizures and status epilepticus (a)** Graphical representation of abnormal results in calcium profiling investigations in the cohort of patients at different time points, demonstrating intra- and inter-patient variability typical in mosaic disease. **(b)** Correlation between age and serum calcium corrected to albumin from the patients' cohort. Red and blue dots correspond to serum calcium measurements below or above normal range, respectively. Linear regression analysis showed a statistically significant negative correlation ($p<0.001$). **(c)** Correlation between occurrence of seizures and serum ionised calcium corrected to pH from the patients' cohort. The scatter plot shows the mean of the two groups, and red dots correspond to ionised calcium measurements below normal range. Linear regression analysis showed a statistically significant correlation ($p=0.013$), independent of the effect of age. **(d)** Correlation between status epilepticus and serum ionised calcium corrected to pH in the patients' cohort. The scatter plot shows the mean of the two groups, and red dots correspond to ionised calcium measurements below normal range. Linear regression analysis showed statistically significant correlation ($p=0.017$), independent of the effect of age.

Figure 3 **- Localised intravascular, perivascular and parenchymal patterns of mineral (calcium) deposition. (a)** Image of the cortex with extensive foci of mineralisation. **(b)** A small cortical vessel (likely to be a capillary) with granular mineralisation of the wall. (**c)** A white matter vessel encircled by mineral and fibrosis. **(d)** A white matter vessel with perivascular deposits and granular parenchymal mineral deposits. In each image, the arrow indicates an example of the mineral deposits.

TABLE

Table 1 **- Patient deep phenotyping and serum calcium metabolic profile in SWS and PPV-DM**
*indicates a patient previously reported in Polubothu et al., 2020

Patient No.	Sex	Age, years	Genotype	Cutaneous features	Neurological features	Ophthalmological features	Other clinical findings	Age at most recent brain MRI, years	Most recent brain MRI findings	Ionised calcium	PTH
1	F	3.8	*GNAQ* c.548G>A, p.R183Q	CM face (right, including forehead)	Seizures, stroke-like episodes and headaches. Normal development	Left increased IOP and choroidal haemangioma	-	3.6	LA left frontal and temporal lobes associated with cortical calcifications. Underdevelopment of left hemispheric superficial cortical veins, enlargement of left deep medullary veins and osteohypertrophy on the left. Generalised parenchymal volume loss in the left cerebral hemisphere. Prominent left cerebellar vessels	Normal	Normal
2	M	3.1	*GNAQ* and *GNA11* WT	No vascular or pigmentary lesions	Seizures, stroke-like episodes, left hemiplegia. Normal development	Normal	-	2.9	LA right parietal lobe associated with subjacent parenchymal volume loss and gyriform calcifications. Slight enlargement of the right choroid plexus	Normal	Normal
3	M	16.1	*GNAQ* c.548G>A, p.R183Q	CM face (bilateral, including forehead) and neck	Intellectual disability, autism and ADHD	Left glaucoma and bilateral choroidal haemangiomas	Joint hypermobility and muscle weakness	14.8	LA right parietal, occipital and temporal lobes. Prominent and atypical veins in the right hemisphere and right cerebellum. Progressive volume loss of cerebellar hemispheres	Normal	Low
4	F	4.0	-	CM right forehead	None	Right glaucoma	-	1.2	LA right occipital and temporal lobes. Abnormal venous drainage in the DMVs territory. Abnormal vessels on the right sylvian fissure and choroid plexus suggestive of DVA	Normal	Normal
5	M	15.9	-	CM face (bilateral, including forehead), neck, upper trunk, and lower limbs	Seizures, left hemiplegia, severe intellectual disability, autism and language disorder	Bilateral glaucoma	Left hip subluxation and valgus deformity of left knee (with overlying vascular	13.1	LA right hemisphere associated with cerebral atrophy and gyriform calcifications. Left cerebellar leptomeningeal angiomatosis	Low	Normal

							lesions on the skin)				
6	M	2.7	-	CM face (bilateral, including forehead)	None	Left buphthalmos, left glaucoma and cloudy cornea	-	0.03	Prominent left cortical and leptomeningeal vessels	Normal	Normal
7	F	11.0	*GNAQ* c.548G>A, p.R183Q	CM face (bilateral, including forehead) and scalp	Seizures, left hemiplegia, headaches, intellectual disability, autism, ADHD and language disorder	Bilateral glaucoma	Scoliosis and leg length discrepancy (with no overlying vascular lesions)	1.9	LA right hemisphere with progression of subjacent cerebral atrophy. LA left frontal lobe, insular cortex and mid brain	-	Normal
8	M	1.9	*GNAQ* c.548G>A, p.R183Q	CM face (bilateral, including forehead) right upper limb and right abdomen associated with overgrowth	Seizures, stroke-like episodes and left hemiplegia. Normal development	Normal	Coronal hypospadias and right hydrocele	1.7	LA right frontal and parietal lobes associated with calcifications on the frontal lobe. Prominent draining DMVs frontal lobe and left insula	Normal	Normal
9	F	11.8	*GNAQ* c.548G>A, p.R183Q	CM face (bilateral, including forehead), neck and upper trunk	Seizures, right hemiplegia, headaches, intellectual disability, autism, ADHD and language disorder	Left glaucoma	Scoliosis. Cervicothoracic lipoma	9.6	LA left hemisphere with subjacent parenchymal volume loss and multiple draining veins. Enhancement of the brainstem.	Low	Normal
10	M	11.6	*GNAQ* c.548G>A, p.R183Q	CM left forehead	Seizures, right hemiplegia, headaches, intellectual disability, autism, ADHD and language disorder	Normal	Recurrent epistaxis	7.7	LA left hemisphere with subjacent parenchymal volume loss. Increased draining veins within the ventricles, cortical signal change and enhancement	Normal	Normal
11	M	15.0	-	Bony prominence left forehead. No vascular or pigmentary lesions on skin	Seizures, headaches, anxiety. Normal development	Right homonymous hemianopia	-	15.0	LA left temporal, parietal and occipital lobes with subjacent parenchymal volume loss and gyriform calcifications. Progression of thickening and bone expansion of the diploic spaces of the left frontal bone	Low	Normal
12	M	2.4	-	CM face (left, including forehead)	Seizures, developmental impairment and social communication difficulties	Left glaucoma and left choroidal haemangioma	-	0.3	LA left parietal and occipital lobes with subjacent parenchymal volume loss. Choroid plexus asymmetry	-	Normal

13	F	9.2	*GNAQ* c.548G>A, p.R183Q	CM face (bilateral, including forehead), trunk and lower limb	Seizures, cerebral palsy of 4 limbs and intellectual disability	Bilateral glaucoma	Microcephaly	6.5	LA both frontal and parietal lobes and left temporal lobe associated with calcifications. Thickening of the skull and prominent deep cerebral DVAs (predominantly on the right)	Normal	Normal
14	F	9.4	*GNAQ* c.548G>A, p.R183Q	CM left forehead	Seizures, right hemiplegia, intellectual disability, autism, ADHD and language disorder	Left increased IOP	-	9.4	LA left frontal, parietal and occipital lobes with subjacent parenchymal volume loss and gyriform calcifications	Low	Normal
15	M	11.8	*GNAQ* c.548G>A, p.R183Q	CM face (bilateral, including forehead), scalp, trunk and limbs associated with overgrowth	Seizures, cerebral palsy of 4 limbs and intellectual disability	Bilateral glaucoma	Scoliosis. Left hip dysplasia and dislocation (with overlying vascular lesions on the skin)	9.6	No imaging available	Normal	Normal
16	M	1.4	-	CM forehead (bilateral) and scalp	Seizures, right hemiplegia and developmental impairment	Bilateral increased IOP		1.6	LA both parietal lobes and right frontal lobe with calcifications. Prominent deep veins along lateral ventricles, left hippocampus, midbrain and the midline. Bilateral enlargement of choroid plexus	-	-
17	F	4.0	-	CM face (left, including forehead), scalp and neck	None	Visual field defect	-	0.4	LA left occipital lobe. Enlargement of left choroid plexus	Normal	Normal
18	F	0.7	*GNAQ* c.548G>A, p.R183Q	CM right forehead	Seizures, right hemiplegia and developmental impairment	Normal	-	0.7	LA right parietal and temporal lobes associated with subjacent parenchymal volume loss and gyriform calcifications. Enlargement of right choroid plexus	Normal	High
19	M	10.9	*GNAQ* c.548G>A, p.R183Q	CM face (left, including forehead), trunk and limbs associated with overgrowth	Seizures, stroke-like episodes, intellectual disability, autism, ADHD and language disorder	Left glaucoma	Myasthenia gravis	10.8	LA parietal, temporal and occipital lobes. Encephalomalacia related to left hemispheric temporo-parietal-occipital disconnection and anterior temporal lobectomy	Low	Normal
20	M	10.8	-	CM face (bilateral, including forehead), neck and upper trunk. Café-au-lait macule neck	Seizures and headaches. Normal development	Left glaucoma	Obesity, acanthosis nigricans, gynaecomastia and isolated adrenarche.	7.8	LA left temporal, parietal and occipital lobes with subjacent parenchymal volume loss and gyriform calcifications. Large transmantle vein on the left extending to enlarged choroid plexus and DVA	Low	Normal

							Hypomineralis-ed dentition				
21	M	5.5	*GNAQ* and *GNA11* WT	CM face (left, including forehead), neck and upper trunk	Stroke-like episodes. Social communication difficulties	Normal	-	3.7	LA left cerebellar hemisphere associated with a large DVA	Low	Normal
22	M	11.2	*GNAQ* c.548G>A, p.R183Q	CM right forehead	Seizures, left hemiplegia, intellectual disability, autism and ADHD	Right glaucoma and left homonymous hemianopia	Scoliosis	6.8	LA right hemisphere with calcifications. Signs of right functional hemispherectomy with shrinkage of the right cerebral hemisphere and mature cystic leukomalacia.	Low	Normal
23	M	13.7	*GNAQ* c.548G>A, p.R183Q	CM face (bilateral, including forehead) and neck	Seizures, stroke-like episodes, headaches, intellectual disability and language disorder	Right glaucoma	-	10.5	LA right frontal lobe with gyriform calcifications	Low	High
24	F	10.3	*GNAQ* c.548G>A, p.R183Q	CM face (bilateral, including forehead), neck, upper trunk and limb associated with overgrowth	Headaches, intellectual disability and language disorder	Left glaucoma	-	7.1	LA right temporal lobe, occipital lobes, splenium of corpus callosum, midbrain and pons. Multiple DVAs in supra- and infra-tentorial compartments	Normal	Normal
25	F	9.6	-	CM face (bilateral, including forehead), neck, buttock and lower limb associated with overgrowth	Seizures, left hemiplegia, intellectual disability, autism, language disorder and dyslexia	Normal	-	6.4	LA right parietal and occipital lobes with calcifications. Signs of disconnection surgery and likely residual connection medially in the right parietal lobe	Low	Normal
26	F	6.00	*GNAQ* c.548G>A, p.R183Q	CM face (bilateral, including forehead), neck, trunk and limbs associated with overgrowth	Seizures, left hemiplegia, intellectual disability and autism	Right glaucoma	-	5.9	LA right cerebral hemisphere. Enlargement of right choroid plexus	Normal	Normal
27	F	2.4	*GNAQ* c.548G>A, p.R183Q	CM right forehead	Seizures. Normal development	Normal	-	2.4	LA right parietal, temporal, and occipital lobes with calcifications. Enlargement of right choroid plexus	Low	High
28	F	15.4	-	CM face (left, including forehead) and scalp	Seizures, right hemiplegia, headaches, language disorder, intellectual disability	Left glaucoma and left choroidal haemangioma	-	11.2	LA left frontal, parietal and temporal lobes with cerebral atrophy and gyriform calcifications. Enlargement of left choroid plexus. Anomalous draining veins on the right cerebral hemisphere	Low	Normal

29	F	1.3	-	CM face (midline, including forehead)	None	Normal	-	1.2	LA both frontal, parietal and occipital lobes associated with prominent medullary veins		
30	M	5.9	*GNA11* c.547C>T, p.R183C	CM with naevus anaemicus face (right, including forehead), trunk and limbs associated with undergrowth	Learning difficulties, Autism	Normal	Leg length discrepancy (with overlying vascular lesions on the skin)	0.9	Small ill-defined foci of signal abnormality in the right caudate nucleus and the adjacent internal capsule, with some associated focal ex vacuo dilatation of the right frontal horn	Low	Normal
31	M	4.3	*GNAQ* c.548G>A, p.R183Q	CM face (right, including forehead)	Seizures, left hemiplegia, stroke-like episodes, intellectual disability and language disorder	Right glaucoma, right choroidal haemangioma	Microcephaly	2.8	Bilateral supra- and infratentorial leptomeningeal angiomatosis with right frontal and temporal lobes relatively spared. Enlargement of right choroid plexus. Bilateral gyriform calcifications in the right temporoparietal and left parietal lobes. Anomalous draining veins more prominent	Low	High
32*	F	10.5	*GNA11* c.547C>T, p.R183C	CM face (bilateral, no forehead involvement), trunk and limbs associated with undergrowth	None	Right iris heterochromia. Right increased IOP	Leg length discrepancy (with overlying vascular lesions on the skin)	6.7	Normal brain findings	Normal	Normal
33*	F	8.4	*GNA11* c.547C>T, p.R183C	CM and extensive dermal melanocytosis face (including forehead), trunk and limbs associated with overgrowth	Seizures, right hemiplegia, intellectual disability and language disorder	Bilateral glaucoma		8.7	LA left hemisphere, right frontal lobe and cerebellar hemisphere. Cortical calcifications left cerebral cortex and right frontal lobe	Normal	Normal
34*	F	7.6	*GNAQ* c.548G>A, p.R183Q	CM trunk and limbs associated with overgrowth. Dermal melanocytosis lower back and café-au-lait macule lower limb	None	Conjunctival melanosis	-	3.2	Normal brain findings	Normal	Normal

35*	F	14.3	*GNAQ* and *GNA11* WT	CM trunk and limbs. Dermal melanocytosis lower back. Café-au-lait macule, lower limb	None	Normal	Recurrent epistaxis	-	Brain MRI not performed*	-	High
36	F	6.3	*GNA11* c.547C>T, p.R183C	CM with naevus anaemicus face (bilateral, including forehead), trunk and limbs associated with overgrowth. Café-au-lait macular pigmentation, trunk	Language difficulties	Normal	-	6.0	Small cortical hyperintensity in right parietal lobe, without diffusion restriction or abnormal enhancement and overlying calvarial thinning. No other intracranial abnormalities	Low	Normal
37*	M	3.8	*GNA11* c.547C>T, p.R183C	CM with naevus anaemicus face (right, including forehead), upper trunk and limbs. Extensive dermal melanocytosis, trunk and limbs	None	Bilateral glaucoma	-	0.7	Suspected calcifications, lateral wall of left lateral ventricle. No focal abnormality or areas of abnormal contrast enhancement	-	Normal
38*	M	12.6	*GNAQ* c.548G>A, p.R183Q	CM face (no forehead involvement), upper trunk and limbs associated with overgrowth. Naevus anaemicus left foot. Extensive dermal melanocytosis, trunk and limbs	ADHD	Normal	-	-	Brain MRI not performed*	Low	Normal
39	F	2.0	*GNAQ* c.548G>A, p.R183Q	CM upper trunk and upper limb. Extensive dermal melanocytosis, trunk and limbs	None	Normal	-	-	Brain MRI not performed*	Normal	Normal
40	M	9.8	*GNA11* c.547C>T, p.R183C	CM trunk and limbs associated with naevus anaemicus and undergrowth. Café-au-lait	Intellectual disability, autism and language disorder	Normal	Leg length discrepancy (with overlying vascular lesions on the skin)	3.1	Normal brain findings	Normal	High

				macular pigmentation neck							
41	F	1.5	-	CM trunk and lower limbs associated with naevus anaemicus and overgrowth.	None	Normal	-	-	Brain MRI not performed*	Normal	High
42	M	0.2	-	CM face (bilateral, including forehead), trunk and upper limb	None	Right glaucoma	-	0.02	LA right frontoparietal and occipital lobes. Enlargement of right choroid plexus	Normal	Normal

Abbreviations: MRI, magnetic resonance imaging; F, female; M, male; WT, wild-type; CM, capillary malformation; ADHD, attention deficit hyperactivity disorder; IOP, intraocular pressure; LA, leptomeningeal angiomatosis; DVA, developmental venous anomaly; DMV, deep medullary vein; PTH, parathyroid hormone

Ionised calcium levels were corrected to pH. Paediatric range references of ionised calcium: 1.15-1.41 mmol/L (< 2 years), 1.19-1.37 mmol/L (2-5 years), 1.22-1.31 mmol/L (5-15 years). PTH reference range: 0.7 - 5.6 pmol/L. Results refer to the first measurements.

According to published guidelines(Waelchli et al., 2014), we currently do not perform MRI/MRA in the absence of vascular lesions on the forehead area and neurological symptoms.

Figure 1

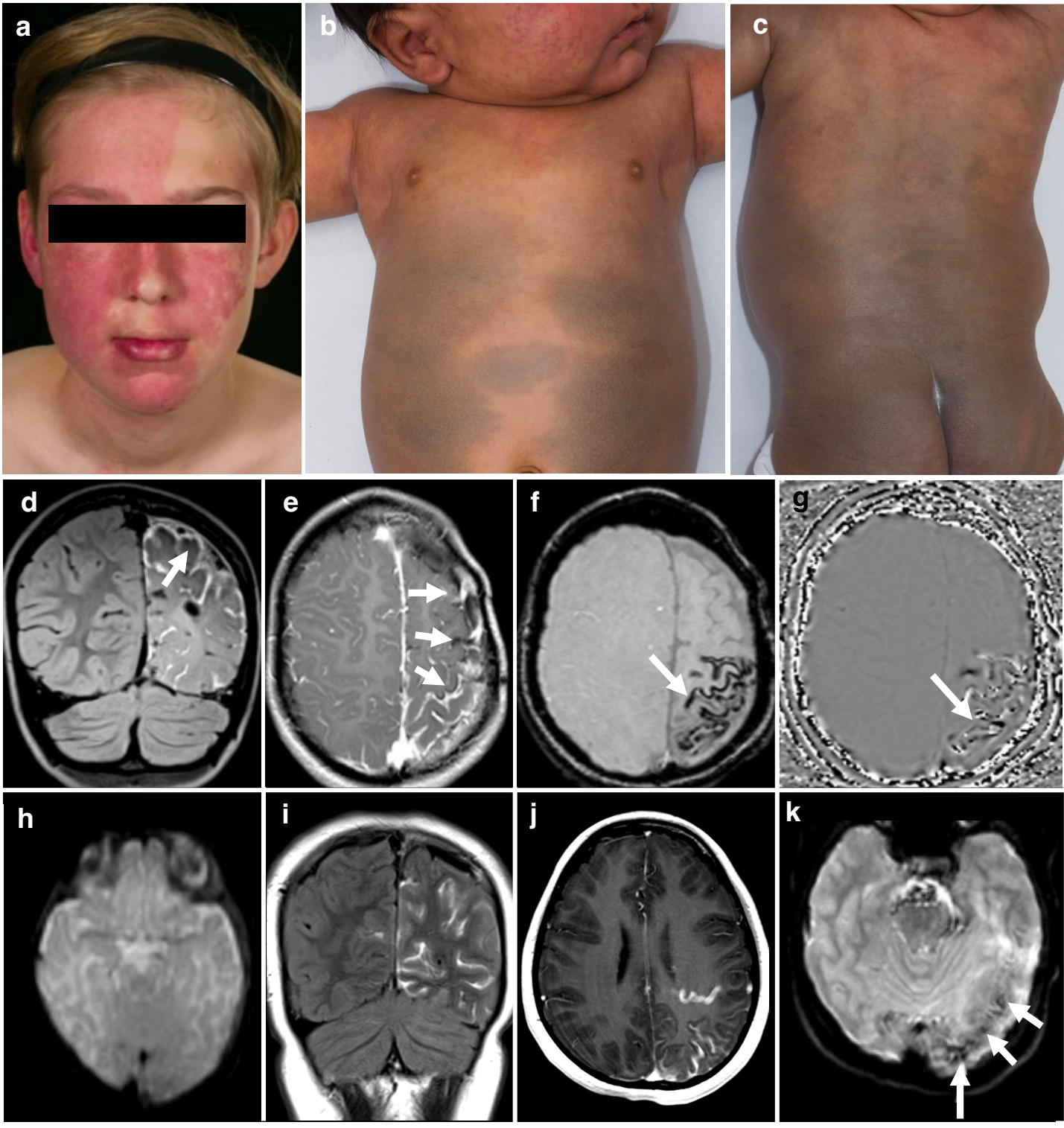

Figure 1 - **Phenotyping and radiological findings in *GNAQ/GNA11* mosaicism. (a)** Clinical features of a SWS syndrome patient with a capillary malformation of the head involving the critical forehead area, associated with glaucoma in the right eye. This patient had hypocalcaemia with low levels of ionised and total calcium and increased PTH. **(b and c)** Clinical features of a PPV-DM patient exhibiting a capillary malformation (with naevus anaemicus) on the face, upper trunk and extensive areas of dermal melanocytosis. **(d** and **e)** Contrast enhanced FLAIR and T1-weighted MR images of a patient with SWS show left frontal, parietal and occipital pial angiomatosis (vascular malformation, arrows). **(f)** Susceptibility-weighted imaging (SWI) and (**g**) SWI phase map depicting vascular calcifications (arrow). This patient had low levels of ionised calcium and total calcium with PTH in the normal range. **(h)** Axial DWI b0 image does not show calcifications on the initial MRI study. **(i-k)**, after 8 years time. **(i)** Coronal Fluid-attenuated inversion recovery (FLAIR) after administration of a gadolinium-based contrast agent shows left parietal and occipital (and some contralateral) sulcal enhancement in keeping with pial angioma. **(j)** Axial post-contrast T1-weighted image depicts the sulcal enhancement and a prominent draining vein. **(k)**. DWI b0 image at follow-up shows foci of increased susceptibility which are suggestive of calcification. Patients and/or parents/guardians provided written consent for the publication of images.

Figure 2

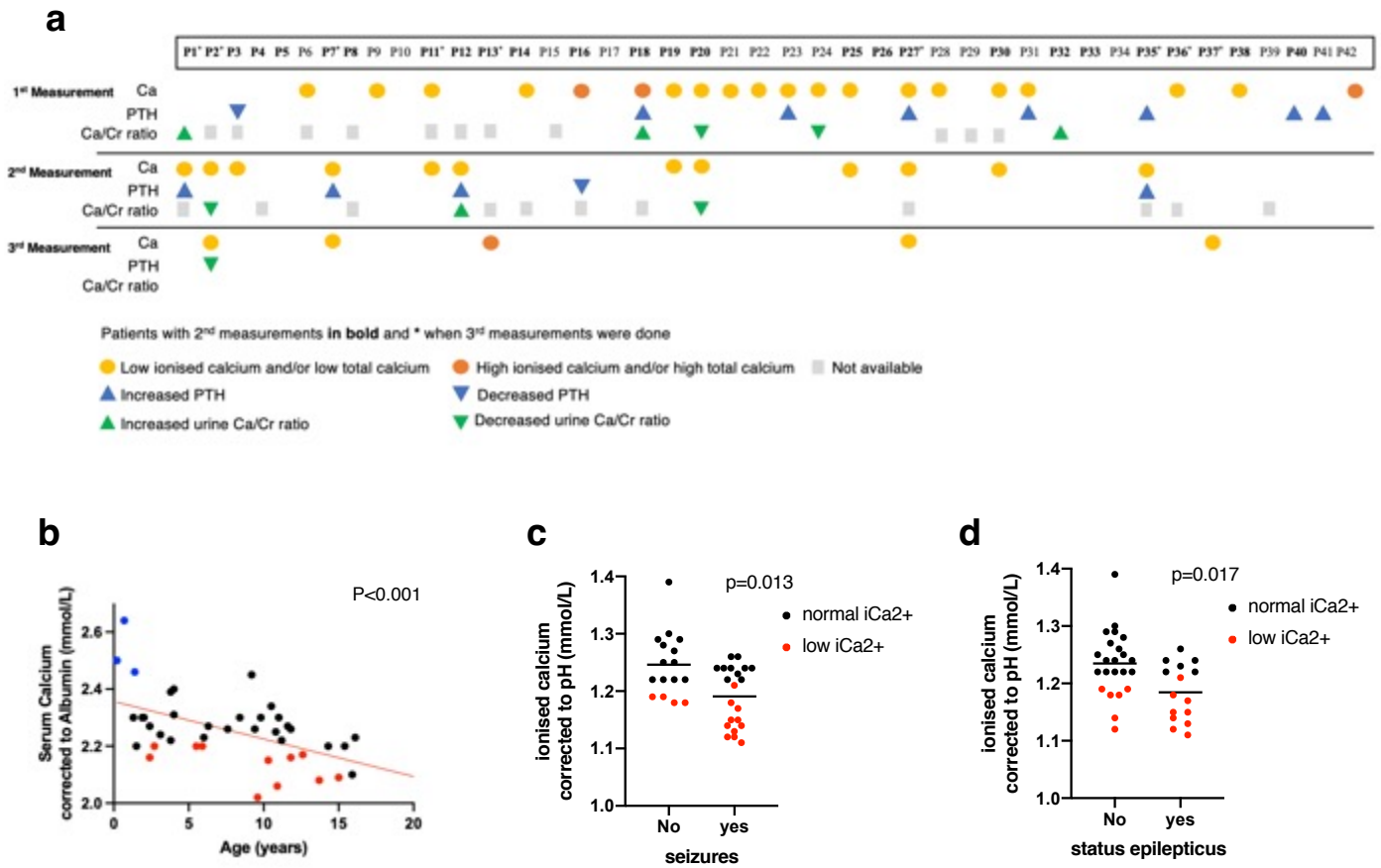

Figure 2 - **Disruption of calcium homeostasis in patients with *GNAQ/GNA11* mosaicism and its association with seizures and status epilepticus (a)** Graphical representation of abnormal results in calcium profiling investigations in the cohort of patients at different time points, demonstrating intra- and inter-patient variability typical in mosaic disease. **(b)** Correlation between age and serum calcium corrected to albumin from the patients' cohort. Red and blue dots correspond to serum calcium measurements below or above normal range, respectively. Linear regression analysis showed a statistically significant negative correlation ($p<0.001$). **(c)** Correlation between occurrence of seizures and serum ionised calcium corrected to pH from the patients' cohort. The scatter plot shows the mean of the two groups, and red dots correspond to ionised calcium measurements below normal range. Linear regression analysis showed a statistically significant correlation ($p=0.013$), independent of the effect of age. **(d)** Correlation between status epilepticus and serum ionised calcium corrected to pH in the patients' cohort. The scatter plot shows the mean of the two groups, and red dots correspond to ionised calcium measurements below normal range. Linear regression analysis showed statistically significant correlation ($p=0.017$), independent of the effect of age.

Figure 3

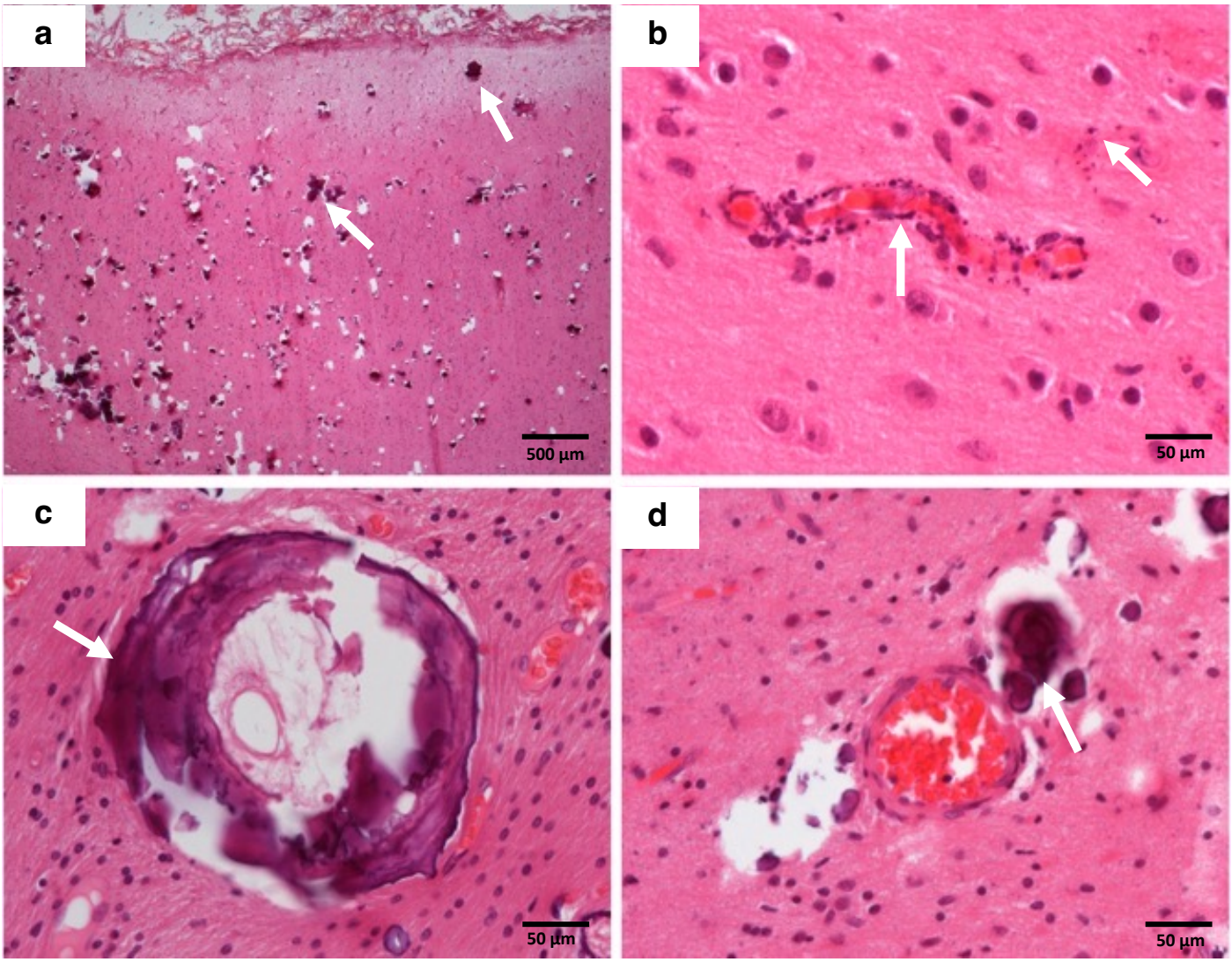

Figure 3 - **Localised intravascular, perivascular and parenchymal patterns of mineral (calcium) deposition. (a)** Image of the cortex with extensive foci of mineralisation. **(b)** A small cortical vessel (likely to be a capillary) with granular mineralisation of the wall. **(c)** A white matter vessel encircled by mineral and fibrosis. **(d)** A white matter vessel with perivascular deposits and granular parenchymal mineral deposits. In each image, the arrow indicates an example of the mineral deposits. Scale bars: A=500 micrometres b, c and d=50 micrometres.

SUPPLEMENTARY MATERIAL OF MANUSCRIPT:

GNAQ/GNA11 mosaicism is associated with abnormal serum calcium indices and microvascular neurocalcification

SUPPLEMENTARY FIGURE LEGENDS

Supplementary Figure 1 **- FGF23 (intact molecule and C-terminal) correlation to 1,25OH Vitamin D, serum calcium corrected to albumin and serum phosphate.** Note the opposite relationships between 1,25-OH Vitamin D and C-terminal FGF23 and its biologically active form intact FGF23. **(a** and **b)** Correlation between intact and C-terminal FGF23 and 1,25OH Vitamin D. **(c** and **d)** Correlation between intact and C-terminal FGF23 and albumin-corrected serum calcium. **(e** and **f)** Correlation between intact and C-terminal FGF23 and serum phosphate. Statistical correlations were performed in Prism as detailed in the methods.

Supplementary Figure 2 **- Calcium homeostatic relationships governed by the parathyroid and kidney behave normally in the *GNAQ/GNA11* mosaic cohort. (a)** Significant inverse correlation between serum calcium corrected to albumin and serum PTH. **(b)** Significant correlation between serum calcium corrected to albumin and urine calcium/creatinine ratio. **(c)** Significant correlation between 1,25OH Vitamin D and intact FGF23. **(d)** Correlation between 1,25OH Vitamin D and PTH. Statistical correlations were performed in Prism as detailed in the methods.

SUPPLEMENTARY TABLES

Supplementary Table 1 **- Systemic calcium metabolic profiling in patients with SWS and PPV-DM**

Supplementary Table 1 Legend:

Abbreviations: WT, wild-type; PTH, Parathyroid hormone; cFGF23, C-terminal fragment fibroblast growth factor 23; iFGF23, intact molecule fibroblast growth factor 23; TRP, intact tubular reabsorption of phosphate; TmP/GFR, ratio of tubular maximum reabsorption of phosphate to glomerular filtration rate and E-GFR, estimated glomerular filtration rate.

Repeat measurements from the same patient are shown on a darker background. All statistical testing was done on values post Vitamin D supplementation and normalisation in the few cases where this was required. Ionised calcium was corrected to pH and total calcium to Albumin. Age-adjusted ionised calcium reference ranges: 1.15-1.41 mmol/L (< 2y), 1.19-1.37 mmol/L (2-5y), 1.22-1.31 mmol/L (5-15y). Age-adjusted total calcium reference ranges: 1.96-2.66 mmol/L (0-5d), 2.17-2.44 mmol/L (5d-3y), 2.22-2.51 mmol/L (3-10y), 2.19-2.66 mmol/L (10-15y), 2.10-2.55 mmol/L (>15y). Age-adjusted phosphate reference ranges: 1.5-2.6 mmol/L (0-5d), 1.2-2.1 mmol/L (5d-3y), 1.2-1.8 mmol/L (3-10y), 1.1-1.75 mmol/L (10-15y), 0.8-1.45 mmol/L (>15y). PTH reference range: 0.7-5.6 pmol/L. Age- and sex-adjusted ALP reference ranges: Female - 65-270 U/L (1-7d), 65-365 U/L (7d-1m), 80-425 U/L (1-3m), 80-345 U/L (3-6m); 60-330 U/L (6-12m), 145-320 U/L (1-3y), 150-380 U/L (3-6y), 175-420 U/L (6-9y), 130-560 U/L (9-11y), 105-420 U/L (11-13y), 70-230 U/L (13-15y), 30-126 U/L (>15y). Male - 65-270 U/L (1-7d), 65-365 U/L (7d-1m), 80-425 U/L (1-3m), 80-345 U/L (3-6m); 60-330 U/L (6-12m), 145-320 U/L (1-3y), 150-380 U/L (3-6y), 175-420 U/L (6-9y), 135-530 U/L (9-11y), 200-495 U/L (11-13y), 130-525 U/L (13-15y), 30-126 U/L (>15y). 25-hydroxy-vitamin D reference range: insufficiency (25-50 nmol/L), deficiency (<25 nmol/L). 1,25-dihydroxy-vitamin D reference range: 108-246 pmol/L. FGF23 (C-terminal fragment) reference range: < 100 RU/ml. FGF23 (intact molecule) reference range: 33-100 pg/mL. TRP reference range: 70-100%. Age-adjusted TmP/GFR reference ranges: 1.55-2.97 mmol/L (newborns), 1.07 – 2.23 mmol/L (1m-2y), 1.10 – 1.88 mmol/L (2-12y), 0.93 – 1.71 mmol/L (12-16y), 0.88 – 1.26 mmol/L (>16y). EGFR for children and adolescents using Bedside Schwartz Formula (ml/min/1.73m^2)

Supplementary Table 2 **- Systemic calcium metabolic profiling in patients with SWS and PPV-DM and antiepileptic treatment**

SUPPLEMENTARY MATERIAL OF MANUSCRIPT:

GNAQ/GNA11 mosaicism is associated with abnormal serum calcium indices and microvascular neurocalcification

Supplementary Table 1 **- Systemic calcium metabolic profiling in patients with SWS and PPV-DM**

Patient No.	**Gender**	**Genotype**	**Age, years**	**Ionised calcium**	**Total calcium**	**Phosphate**	**PTH**	**ALP**	**25-hydroxy-vitamin D**	**1,25-dihydroxy-vitamin D**	**FGF23 (c-terminal fragment)**	**FGF23 (intact molecule)**	**Urine Ca/Cr ratio**	**TRP (%)**	**TmP/GFR**	**E-GFR**
1	F	*GNAQ* c.548G>A, p.R183Q	3.8	1.23	2.39	1.33	1.6	221	89	-	-	-	Increased	-	-	90.2
			4.8	1.03 (low)	2.00 (low)	1.66	8.3 (high)	177	94	-	69	55.4	-	-	-	107.8
			5.3	1.25	2.30	1.64	1.5	154	95	126	-	-	Normal	85.8	1.41	80.8
2	M	*GNAQ* and *GNA11* WT	3.1	1.24	2.24	1.59	1.5	236	72	-	-	-	-			-
			4.3	1.10 (low)	2.10 (low)	1.88 (high)	5.6	196	107	149	74	39.3	Decreased	91.4	1.72	-
			4.8	1.21	2.20 (low)	1.58	0.3 (low)	164	101	-	-	-	Normal	94.1	1.49	112.8
3	M	*GNAQ* c.548G>A, p.R183Q	16.1	1.22	2.23	1.04	0.3 (low)	146 (high)	53	-	-	-	-	-	-	70.7
			17.2	1.19 (low)	2.20	0.98	1.8	103	76	100 (low)	79	56.9	Normal	95.8	1.28	82.2
4	F	-	4.0	1.22	2.40	1.32	4.4	239	95	-	-	-	Normal	-	-	-

			5.0	1.26	2.30	1.47	5.5	186	105	-	71	-	-	-	-	120.9
5	M	-	15.9	1.24	2.1	0.98	1.3	78	174	-	-	-	Normal	-	-	128.6
			17.4	1.21	2.20	1.04	2.3	76	67	77 (low)	-	-	Normal	91.3	0.95	106.2
6	M	-	2.7	1.22	2.20 (low)	1.54	3.5	109 (low)	79	-	-	-	-	-	-	94.1
7	F	*GNAQ* c.548G>A, p.R183Q	11.0	-	2.30	1.53	4.8	300	57	-	-	-	Normal	-	-	136.1
			12.1	1.19 (low)	2.20	1.54	6.1 (high)	245	107	174	-	-	Normal	93.8	1.44	120.1
			12.4	1.20 (low)	2.20	1.64	3.2	238	85	138	84	43.9	Normal	96.5	1.58	97.36
8	M	*GNAQ* c.548G>A, p.R183Q	1.9	1.24	2.30	1.58	3.0	175	97	-	-		-	-	-	-
			3.1	1.19	2.30	1.78	1.5	417 (high)	83	109	355 (high)	59.2	-	-	-	133.9
9	F	*GNAQ* c.548G>A, p.R183Q	11.8	1.12 (low)	2.16 (low)	1.45	2.6	174	78	-	-	-	Normal	-	-	122.6
10	M	*GNAQ* c.548G>A, p.R183Q	11.6	1.22	2.27	1.34	0.8	306	81	-	-	-	Normal	-	-	114.4
11	M	-	15.0	1.13 (low)	2.09 (low)	1.20	4.4	86 (low)	57	-	-	-	Normal	-	-	127.1
			16.0	1.19 (low)	2.10	1.4	2.1	70	79	63 (low)	63	56.5	Normal	97.2	1.36	137.3
			16.5	1.20	2.20	1.21	2.0	62	-	53 (low)	-	-	Normal	98.3	1.19	100.2

12	M	-	2.4	-	2.27	1.59	1.4	139 (low)	90	-	-	-	-	-	-	122.4
			3.6	1.19	2.20 (low)	1.76	9.9 (high)	140 (low)	117	97 (low)	43	-	Increased	85.8	1.51	73.47
13	F	*GNAQ* c.548G>A, p.R183Q	9.2	1.26	2.45	1.05 (low)	3.0	132	118	-	-	-	-	-	-	125.5
			10.2	1.31	2.5	1.19	3.2	163	125	140	124 (high)	76.5	-	-	-	105.4
			10.5	1.32 (high)	2.4	1.28	3.3	160	105	-	68	82.3	-	-	-	112.3
14	F	*GNAQ* c.548G>A, p.R183Q	9.4	1.17 (low)	2.26	1.57	4.4	128 (low)	66	-	-	-	Normal	-	-	108.9
			10.6	1.25	2.20	1.45	1.0	130	87	99 (low)	-	-	-	-	-	-
15	M	*GNAQ* c.548G>A, p.R183Q	11.8	1.22	2.26	1.29	4.4	171 (low)	111	-	-	-	-	-	-	-
16	M	-	1.4	-	2.46 (high)	1.58	0.9	317	114	-	-	-	-	-	-	-
			2.7	1.22	2.30	1.43	0.6 (low)	259	131	145	23	33.7	-	-	--	83.3
17	F	-	4.0	1.25	2.31	1.52	1.6	217	81	-	-	-	Normal	-	-	92.61
18	F	*GNAQ* c.548G>A, p.R183Q	0.7	1.26	2.64 (high)	1.77	8.9 (high)	171	130	-	-	-	Increased	-	-	-
			1.1	-	2.30	2.21 (high)	-	225	122	-	-	-	-	-	-	97.16
19	M	*GNAQ* c.548G>A, p.R183Q	10.9	1.15 (low)	2.06 (low)	1.37	2.4	198	97	-	-	-	Normal	-	-	121.64

			12.3	1.19 (low)	2.10 (low)	1.74	2.2	103 (low)	51	102 (low)	-	-	Normal	98.9	1.72	148.1
20	M	-	10.8	1.18 (low)	2.25	1.71	1.5	154	62	-	-	-	Decreased	-	-	181.6
			12.1	1.20 (low)	2.20	1.64	0.9	137 (low)	60	-	-	-	Decreased	-	-	133.3
21	M	*GNAQ* and *GNA11* WT	5.5	1.19 (low)	2.20 (low)	1.54	4.5	277	70	-	-	-	Normal	-	-	135.6
22	M	*GNAQ* c.548G>A, p.R183Q	11.2	1.21 (low)	2.22	1.65	1.5	197 (low)	82	-	-	-	Normal	-	-	152.6
23	M	*GNAQ* c.548G>A, p.R183Q	13.7	1.15 (low)	2.08 (low)	1.50	7.4 (high)	353	55	-	-	-	Normal	-	-	105.9
24	F	*GNAQ* c.548G>A, p.R183Q	10.3	1.25	2.15 (low)	1.30	2.3	279	97	-	-	-	Decreased	-	-	122.12
25	F	-	9.6	1.14 (low)	2.02 (low)	1.46	4.8	205	64	-	-	-	Normal	-	-	137.5
			10.5	0.78 (low)	1.90 (low)	2.00 (high)	3.5	230	88	128	35	73.2	Normal	93.8	1.88	114.9
			10.9	1.15 (low)	2.0 (low)	1.51	1.9	302	80	103 (low)	-	-	Normal	92.1	1.39	111.9
26	F	*GNAQ* c.548G>A,	6.00	1.24	2.23	1.56	2.1	359	60		-	-	Normal	-	-	146.0

		p.R183Q	6.8	1.28	2.30	1.49	3.3	462 (high)	73	218	-	-	Normal	96.5	1.44	159.56
27	F	*GNAQ* c.548G>A, p.R183Q	2.4	1.14 (low)	2.16 (low)	1.62	5.9 (high)	226	132		-	-	Normal	-	-	-
			3.3	1.19	2.20 (low)	1.49	5.1	253	135	196	167 (high)	24.9	-	-	-	120.21
			3.8	1.25	2.20 (low)	1.49	0.8	258	116	139	-	-	Normal	97.6	1.38	-
28	F	-	15.4	1.11 (low)	2.20	1.38	2.30	66	66	-	163 (high)	-	-	-	-	100.2
29	F	-	1.3	1.29	2.30	1.56	3.9	125	85	-	137 (high)	50.9	-	-	-	102.1
30	M	*GNA11* c.547C>T, p.R183C	5.9	1.19 (low)	2.20 (low)	1.81 (high)	3.6	221	80	-	-	-	-	-	-	113.2
			6.7	1.24	2.20 (low)	1.32	1.6	141 (low)	121	-	-	-	Normal	93.8	1.24	148.6
31	M	*GNAQ* c.548G>A, p.R183Q	4.3	1.12 (low)	-	-	6.6 (high)	-	99	-	-	-	Normal	-	-	-
32*	F	*GNA11* c.547C>T, p.R183C	10.5	1.27	2.34	1.29	0.8	248	103	-	-	-	Increased	-	-	112.6
			11.5	-	2.30	1.34	4.3	157	125	201	110 (high)	23.6 (low)	Normal	94.1	1.26	97.3
33*	F	*GNA11* c.547C>T, p.R183C	8.4	1.24	2.30	1.45	1.8	260	52	-	-		Normal	-	-	91.7
			9.1	1.22	2.30	1.38	1.1	228	68	146	-	-	Normal	86.9	1.2	86.1

34*	F	*GNAQ* c.548G>A, p.R183Q	7.6	1.22	2.26	1.56	1.8	170 (low)	65	-	-	-	Normal	-	-	72.5
35*	F	*GNAQ* and *GNA11* WT	14.3	-	2.20	1.23	7.8 (high)	83	58	-	-	-	Normal	-	-	88.8
			14.7	1.20 (low)	2.20	1.31	10.5 (high)	68	35 (low)	-	-	-	-	-	-	93.2
			15.7	1.24	2.10	1.47 (high)	5.0	61	71	-	-	-	Normal	91.4	1.34	90.6
36	F	*GNA11* c.547C>T, p.R183C	6.3	1.18 (low)	2.27	1.58	2.6	218	64	-	-	-	Normal	-	-	103.4
			7.2	1.23	2.30	1.47	2.7	163 (low)	52	-	-	-	-	-	-	116.8
			7.7	1.30	2.30	1.38	3.5	197	71	159	53	44.1	Increased	90.2	1.24	117.6
37*	M	*GNA11* c.547C>T, p.R183C	3.8	-	2.22	1.92 (high)	5.1	193	50	-	-	-	Normal	-	-	-
			4.7	1.26	2.30	1.92 (high)	1.7	166	98	-	137 (high)	-	Normal		-	129.7
			5.1	1.19 (low)	2.30	1.83 (high)	0.7	161	76	134	66	-	Normal	87.5	1.6	109.5
38*	M	*GNAQ* c.548G>A, p.R183Q	12.6	1.18 (low)	2.17 (low)	1.65	3.8	219	75	-	-	-	Normal	-	-	120.8
			13.6	1.22	2.2	1.46	4.3	203	83	113	74	51.8	Normal	91.6	1.34	106.1
39	F	*GNAQ* c.548G>A, p.R183Q	2.0	1.28	2.30	1.66	2.8	185	141	-	134 (high)	52.5	-	-	-	102.0

40	M	*GNA11* c.547C>T, p.R183C	9.8	1.29	2.30	1.53	6.6 (high)	215	92	-	200 (high)	39.0	Normal	-	-	110.7
			10.4	1.26	2.30	1.41	1.9	230	84	122	-	-	Normal	94.2	1.33	108.7
41	F	-	1.5	1.30	2.20	1.96	6.6 (high)	129 (low)	116	138	-	56.3	Normal	86.2	1.69	109.5
42	M	-	0.2	1.39	2.50 (high)	2.21 (high)	1.50	130	99	-	-	-	Normal	86.9	1.92	-

Abbreviations: WT, wild-type; PTH, Parathyroid hormone; cFGF23, C-terminal fragment fibroblast growth factor 23; iFGF23, intact molecule fibroblast growth factor 23; TRP, intact tubular reabsorption of phosphate; TmP/GFR, ratio of tubular maximum reabsorption of phosphate to glomerular filtration rate and E-GFR, estimated glomerular filtration rate.

Repeat measurements from the same patient are shown on a darker background. All statistical testing was done on values post Vitamin D supplementation and normalisation in the few cases where this was required. Ionised calcium was corrected to pH and total calcium to Albumin. Age-adjusted ionised calcium reference ranges: 1.15-1.41 mmol/L (< 2y), 1.19-1.37 mmol/L (2-5y), 1.22-1.31 mmol/L (5-15y). Age-adjusted total calcium reference ranges: 1.96-2.66 mmol/L (0-5d), 2.17-2.44 mmol/L (5d-3y), 2.22-2.51 mmol/L (3-10y), 2.19-2.66 mmol/L (10-15y), 2.10-2.55 mmol/L (>15y). Age-adjusted phosphate reference ranges: 1.5-2.6 mmol/L (0-5d), 1.2-2.1 mmol/L (5d-3y), 1.2-1.8 mmol/L (3-10y), 1.1-1.75 mmol/L (10-15y), 0.8-1.45 mmol/L (>15y). PTH reference range: 0.7-5.6 pmol/L. Age- and sex-adjusted ALP reference ranges: Female - 65-270 U/L (1-7d), 65-365 U/L (7d-1m), 80-425 U/L (1-3m), 80-345 U/L (3-6m); 60-330 U/L (6-12m), 145-320 U/L (1-3y), 150-380 U/L (3-6y), 175-420 U/L (6-9y), 130-560 U/L (9-11y), 105-420 U/L (11-13y), 70-230 U/L (13-15y), 30-126 U/L (>15y). Male - 65-270 U/L (1-7d), 65-365 U/L (7d-1m), 80-425 U/L (1-3m), 80-345 U/L (3-6m); 60-330 U/L (6-12m), 145-320 U/L (1-3y), 150-380 U/L (3-6y), 175-420 U/L (6-9y), 135-530 U/L (9-11y), 200-495 U/L (11-13y), 130-525 U/L (13-15y), 30-126 U/L (>15y). 25-hydroxy-vitamin D reference range: insufficiency (25-50 nmol/L), deficiency (<25 nmol/L). 1,25-dihydroxy-vitamin D reference range: 108-246 pmol/L. FGF23 (C-terminal fragment) reference range: < 100 RU/ml. FGF23 (intact molecule) reference range: 33-100 pg/mL. TRP reference range: 70-100%. Age-adjusted TmP/GFR reference ranges: 1.55-2.97 mmol/L (newborns), 1.07 – 2.23 mmol/L (1m-2y), 1.10 – 1.88 mmol/L (2-12y), 0.93 – 1.71 mmol/L (12-16y), 0.88 – 1.26 mmol/L (>16y). EGFR for children and adolescents using Bedside Schwartz Formula (ml/min/1.73m^2)

SUPPLEMENTARY MATERIAL OF MANUSCRIPT:

GNAQ/GNA11 mosaicism is associated with abnormal serum calcium indices and microvascular neurocalcification

Supplementary Table 2 **- Systemic calcium metabolic profiling in patients with SWS and PPV-DM and antiepileptic treatment**

Patient No.	**Gender**	**Genotype**	**Age, years**	**Ionised calcium**	**Total calcium**	**Phosphate**	**PTH**	**25-hydroxy-vitamin D**	**1,25-dihydroxy-vitamin D**	**FGF23 (c-terminal fragment)**	**FGF23 (intact molecule)**	**Urine Ca/Cr ratio**	**Antiepileptics**
1	F	*GNAQ* c.548G>A, p.R183Q	3.8	1.23	2.39	1.33	1.6	89	-	-	-	Increased	Levetiracetam, zonisamide
			4.8	1.03 (low)	2.00 (low)	1.66	8.3 (high)	94	-	69	55.4	-	
			5.3	1.25	2.30	1.64	1.5	95	126	-	-	Normal	
2	M	*GNAQ* and *GNA11* WT	3.1	1.24	2.24	1.59	1.5	72	-	-	-	-	Levetiracetam, sodium valproate, zonisamide
			4.3	1.10 (low)	2.10 (low)	1.88 (high)	5.6	107	149	74	39.3	Decreased	
			4.8	1.21	2.20 (low)	1.58	0.3 (low)	101	-	-	-	Normal	
3	M	*GNAQ* c.548G>A, p.R183Q	16.1	1.22	2.23	1.04	0.3 (low)	53	-	-	-	-	None
			17.2	1.19 (low)	2.20	0.98	1.8	76	100 (low)	79	56.9	Normal	
4	F	-	4.0	1.22	2.40	1.32	4.4	95	-	-	-	Normal	None
			5.0	1.26	2.30	1.47	5.5	105	-	71	-	-	

5	M	-	15.9	1.24	2.1	0.98	1.3	174	-	-	-	Normal	Carbamazepine
			17.4	1.21	2.20	1.04	2.3	67	77 (low)	-	-	Normal	
6	M	-	2.7	1.22	2.20 (low)	1.54	3.5	79	-	-	-	-	Levetiracetam
7	F	*GNAQ* c.548G>A, p.R183Q	11.0	-	2.30	1.53	4.8	57	-	-	-	Normal	Levetiracetam, oxcarbazepin
			12.1	1.19 (low)	2.20	1.54	6.1 (high)	107	174	-	-	Normal	
			12.4	1.20 (low)	2.20	1.64	3.2	85	138	84	43.9	Normal	
8	M	*GNAQ* c.548G>A, p.R183Q	1.9	1.24	2.30	1.58	3.0	97	-	-	-	-	Levetiracetam
			3.1	1.19	2.30	1.78	1.5	83	109	355 (high)	59.2	-	
9	F	*GNAQ* c.548G>A, p.R183Q	11.8	1.12 (low)	2.16 (low)	1.45	2.6	78	-	-	-	Normal	Levetiracetam, topiramate
10	M	*GNAQ* c.548G>A, p.R183Q	11.6	1.22	2.27	1.34	0.8	81	-	-	-	Normal	Levetiracetam, sodium valproate
11	M	-	15.0	1.13 (low)	2.09 (low)	1.20	4.4	57	-	-	-	Normal	Levetiracetam, sodium valproate, gabapentine
			16.0	1.19 (low)	2.10	1.4	2.1	79	63 (low)	63	56.5	Normal	
			16.5	1.20	2.20	1.21	2.0	-	53 (low)	-	-	Normal	
12	M	-	2.4	-	2.27	1.59	1.4	90	-				Topiramate, clobazam

			3.6	1.19	2.20 (low)	1.76	9.9 (high)	117	97 (low)	43	-	Increased	
13	F	*GNAQ* c.548G>A, p.R183Q	9.2	1.26	2.45	1.05 (low)	3.0	118	-	-	-	-	Levetiracetam, sodium valproate
			10.2	1.31	2.5	1.19	3.2	125	140	124 (high)	76.5	-	
		25.10.22	10.5	1.32 (high)	2.4	1.28	3.3	105	-	68	82.3	-	
14	F	*GNAQ* c.548G>A, p.R183Q	9.4	1.17 (low)	2.26	1.57	4.4	66	-	-	-	Normal	None
			10.6	1.25	2.20	1.45	1.0	87	99 (low)	-	-	-	
15	M	*GNAQ* c.548G>A, p.R183Q	11.8	1.22	2.26	1.29	4.4	111	-	-	-	-	Valproate, carbamazepine
16	M	-	1.4	-	2.46 (high)	1.58	0.9	114	-	-	-	-	Levetiracetam, oxcarbazepine, topiramate
			2.7	1.22	2.30	1.43	0.6 (low)	131	145	23	33.7	-	
17	F	-	4.0	1.25	2.31	1.52	1.6	81	-	-	-	Normal	None
18	F	*GNAQ* c.548G>A, p.R183Q	0.7	1.26	2.64 (high)	1.77	8.9 (high)	130	-	-	-	Increased	Levetiracetam, sodium valproate, oxcarbazepine, topiramate
			1.1	-	2.30	2.21 (high)	-	122	-	-	-	-	
19	M	*GNAQ* c.548G>A, p.R183Q	10.9	1.15 (low)	2.06 (low)	1.37	2.4	97	-	-	-	Normal	Levetiracetam, carbamazepine

			12.3	1.19 (low)	2.10 (low)	1.74	2.2	51	102 (low)	-	-	Normal	Levetiracetam
20	M	-	10.8	1.18 (low)	2.25	1.71	1.5	62	-	-	-	Decreased	Levetiracetam
		24.11	12.1	1.20 (low)	2.20	1.64	0.9	60	-	-	-	Decreased	
21	M	*GNAQ* and *GNA11* WT	5.5	1.19 (low)	2.20 (low)	1.54	4.5	70	-	-	-	Normal	None
22	M	*GNAQ* c.548G>A, p.R183Q	11.2	1.21 (low)	2.22	1.65	1.5	82	-	-	-	Normal	None
23	M	*GNAQ* c.548G>A, p.R183Q	13.7	1.15 (low)	2.08 (low)	1.50	7.4 (high)	55	-	-	-	Normal	Oxcarbazepine, briveracetam
24	F	*GNAQ* c.548G>A, p.R183Q	10.3	1.25	2.15 (low)	1.30	2.3	97	-	-	-	Decreased	Carbamazepine
25	F	-	9.6	1.14 (low)	2.02 (low)	1.46	4.8	64	-	-	-	Normal	Oxcarbazepine, zonisamide
			10.5	0.78 (low)	1.90 (low)	2.00 (high)	3.5	88	128	35	73.2	Normal	
			10.9	1.15 (low)	2.0 (low)	1.51	1.9	80	103 (low)	-	-	Normal	
26	F	*GNAQ* c.548G>A, p.R183Q	6.00	1.24	2.23	1.56	2.1	60	-	-	-	Normal	Levetiracetam
			6.8	1.28	2.30	1.49	3.3	73	218	-	-	Normal	

27	F	*GNAQ* c.548G>A, p.R183Q	2.4	1.14 (low)	2.16 (low)	1.62	5.9 (high)	132	-	-	-	Normal	Levetiracetam, oxcarbazepine, topiramate
			3.3	1.19	2.20 (low)	1.49	5.1	135	196	167 (high)	24.9	-	
			3.8	1.25	2.20 (low)	1.49	0.8	116	139	-	-	Normal	Levetiracetam, oxcarbazepine
28	F	-	15.4	1.11 (low)	2.20	1.38	2.30	66	-	163 (high)	-	-	Levetiracetam
29	F	-	1.3	1.29	2.30	1.56	3.9	85	-	137 (high)	50.9	-	None
30	M	*GNA11* c.547C>T, p.R183C	5.9	1.19 (low)	2.20 (low)	1.81 (high)	3.6	80	-	-	-	-	None
			6.7	1.24	2.20 (low)	1.32	1.6	121	-	-	-	Normal	
31	M	*GNAQ* c.548G>A, p.R183Q	4.3	1.12 (low)	-	-	6.6 (high)	99	-	-	-	Normal	Levetiracetam, oxcarbazepine, zonisamide
32*	F	*GNA11* c.547C>T, p.R183C	10.5	1.27	2.34	1.29	0.8	103	-	-	-	Increased	None
			11.5	-	2.30	1.34	4.3	125	201	110 (high)	23.6 (low)	Normal	
33*	F	*GNA11* c.547C>T, p.R183C	8.4	1.24	2.30	1.45	1.8	52	-	-	-	Normal	Levetiracetam, topiramate
			9.1	1.22	2.30	1.38	1.1	68	146	-	-	Normal	
34*	F	*GNAQ* c.548G>A, p.R183Q	7.6	1.22	2.26	1.56	1.8	65	-	-	-	Normal	None

35*	F	*GNAQ* and *GNA11* WT	14.3	-	2.20	1.23	7.8 (high)	58	-	-	-	Normal	None
			14.7	1.20 (low)	2.20	1.31	10.5 (high)	35 (low)	-	-	-	-	
			15.7	1.24	2.10	1.47 (high)	5.0	71	-	-	-	Normal	
36	F	*GNA11* c.547C>T, p.R183C	6.3	1.18 (low)	2.27	1.58	2.6	64	-	-	-	Normal	None
			7.2	1.23	2.30	1.47	2.7	52	-	-	-	-	
			7.7	1.30	2.30	1.38	3.5	71	159	53	44.1	Increased	
37*	M	*GNA11* c.547C>T, p.R183C	3.8	-	2.22	1.92 (high)	5.1	50	-	-	-	Normal	None
			4.7	1.26	2.30	1.92 (high)	1.7	98	-	137 (high)	-	Normal	
			5.1	1.19 (low)	2.30	1.83 (high)	0.7	76	134	66	-	Normal	
38*	M	*GNAQ* c.548G>A, p.R183Q	12.6	1.18 (low)	2.17 (low)	1.65	3.8	75	-	-	-	Normal	None
			13.6	1.22	2.2	1.46	4.3	83	113	74	51.8	Normal	
39	F	*GNAQ* c.548G>A, p.R183Q	2.0	1.28	2.30	1.66	2.8	141	-	134 (high)	52.5	-	None
40	M	*GNA11* c.547C>T, p.R183C	9.8	1.29	2.30	1.53	6.6 (high)	92	-	200 (high)	39.0	Normal	None
			10.4	1.26	2.30	1.41	1.9	84	122	-	-	Normal	

41	F	-	1.5	1.30	2.20	1.96	6.6 (high)	116	138	-	56.3	Normal	None
42	M	-	0.2	1.39	2.50 (high)	2.21 (high)	1.50	99	-	-	-	Normal	None

Supplementary Figure 1

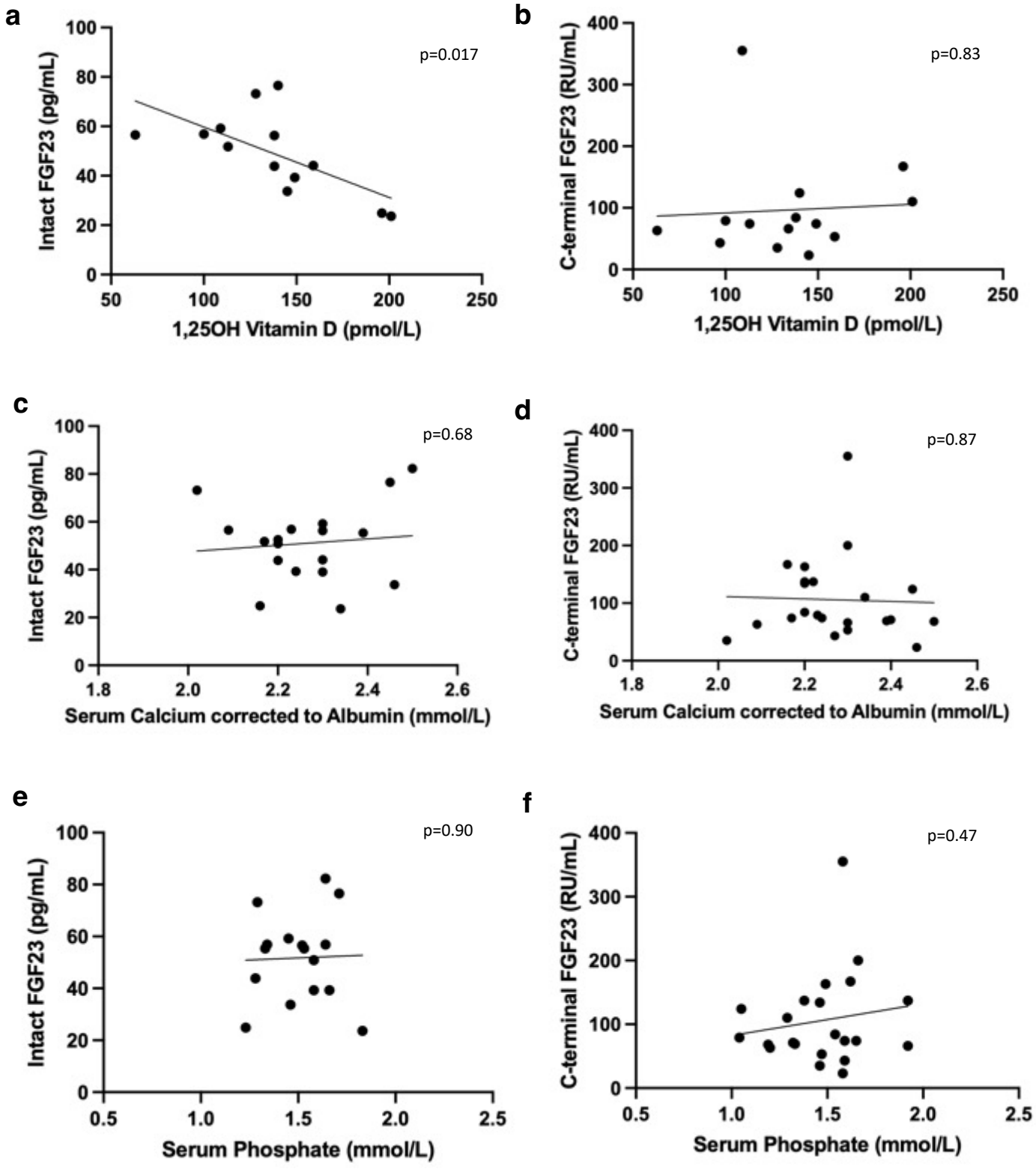

Supplementary Figure 1 **- FGF23 (intact molecule and C-terminal) correlation to 1,25OH Vitamin D, serum calcium corrected to albumin and serum phosphate.** Note the opposite relationships between 1,25-OH Vitamin D and C-terminal FGF23 and its biologically active form intact FGF23. **(a** and **b)** Correlation between intact and C-terminal FGF23 and 1,25OH Vitamin D. **(c** and **d)** Correlation between intact and C-terminal FGF23 and albumin-corrected serum calcium. **(e** and **f)** Correlation between intact and C-terminal FGF23 and serum phosphate. Statistical correlations were performed in Prism as detailed in the methods.

Supplementary Figure 2

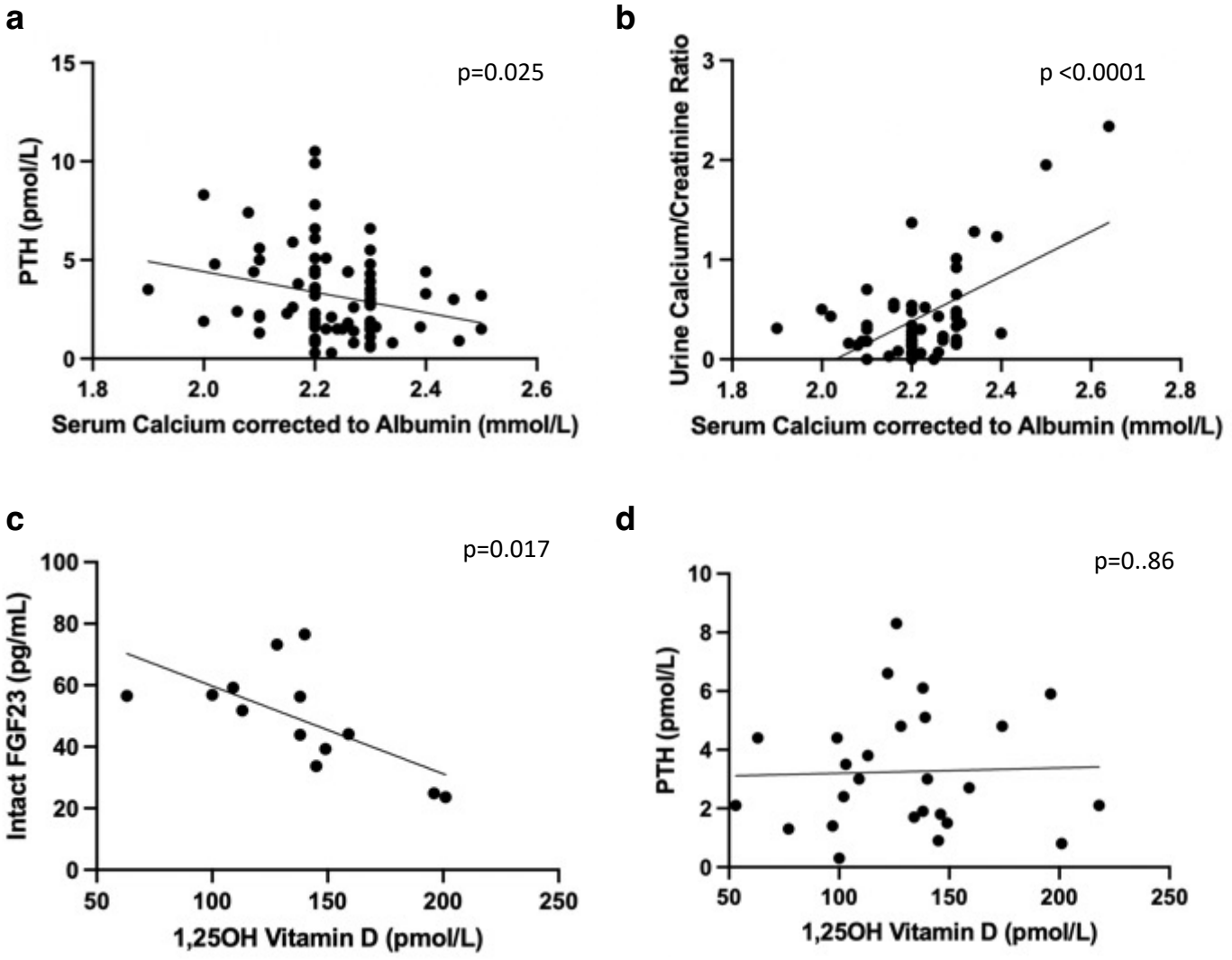

Supplementary Figure 2 **- Calcium homeostatic relationships governed by the parathyroid and kidney behave normally in the *GNAQ/GNA11* mosaic cohort. (a)** Significant inverse correlation between serum calcium corrected to albumin and serum PTH. **(b)** Significant correlation between serum calcium corrected to albumin and urine calcium/creatinine ratio. **(c)** Significant correlation between 1,25OH Vitamin D and intact FGF23. **(d)** Correlation between 1,25OH Vitamin D and PTH. Statistical correlations were performed in Prism as detailed in the methods.